Bulletin of Electrical Engineering and Informatics
Vol. 15, No. 6, December 2026, pp. 4850~4862
ISSN: 2302-9285, DOI: 10.11591/eei.v15i6.13589

Artificial intelligence–based design of proportional-integral controllers for active power filters in railway electrification

Chakrit Panpean[1,2], Chirdpong Deelertpaiboon[1], Jeerawan Homjan[3], Ittiphong Yongyee[3], Warunee Srisongkram[4], Napat Watjanatepin[5]
[1]Department of Instrumentation and Electrical Energy Engineering, Faculty of Engineering, King Mongkut's University of Technology North Bangkok, Bangkok, Thailand
[2]Operations Center of Modern Automotive Technology and Innovation, and Rail Transport Systems, KMUTNB Techno Park, King Mongkut's University of Technology North Bangkok, Bangkok, Thailand
[3]Department of Mechatronics Engineering, Faculty of Engineering and Architecture, Rajamangala University of Technology Suvarnabhumi, Nonthaburi, Thailand
[4]Department of Electrical Engineering, Faculty of Engineering and Architecture, Rajamangala University of Technology Suvarnabhumi, Nonthaburi, Thailand
[5]Department of Electrical Engineering, Faculty of Engineering, Bangkokthonburi University, Bangkok, Thailand

Article Info

Article history:

Received Jun 6, 2026
Revised Sep 17, 2026
Accepted Oct 4, 2026

Keywords:

Active power filters
Adaptive Tabu search
Artificial intelligence
Electric railway systems
Power quality improvement

ABSTRACT

Conventional tuning of proportional–integral (PI) controllers for active power filters (APFs) cannot ensure optimal improvement of power quality performance in electric railway applications. This research introduces an artificial intelligence (AI) methodology for the design of a PI controller in electric railway systems. The adaptive Tabu search (ATS) algorithm is utilized to search for the optimal parameters of a compensating current controller and direct current (DC) bus voltage controller, with the aim of concurrently optimizing harmonic current suppression, current imbalance compensation, and power factor (PF) correction. The efficacy of the proposed method is assessed via hardware-in-the-loop (HIL) simulation. Experimental results validate that the compensating current controller and DC bus voltage controller, designed using the ATS algorithm, demonstrably improve harmonic mitigation performance. This enhancement is substantiated through the power quality index, specifically the percentage of total harmonic distortion of current (%THDi), percentage of current unbalance factor (%CUF), and the PF compliance with the IEEE standard. Consequently, the proposed approach offers a practical and effective solution for elevating power quality within electric railway systems.

This is an open access article under the CC BY-SA license.

Corresponding Author:

Ittiphong Yongyee
Department of Mechatronics Engineering, Faculty of Engineering and Architecture
Rajamangala University of Technology Suvarnabhumi
217 Nonthaburi Road, Suan Yai, Mueang Nonthaburi 11000, Thailand
Email: ittiphong.y@rmutsb.ac.th

1. INTRODUCTION

The rapid expansion of electric railway networks has significantly increased electrical energy demand, making energy efficiency a critical factor in mitigating global warming. Modern railways rely heavily on power electronic devices for traction and passenger services. Because these devices operate with dynamic energy consumption profiles, they introduce highly nonlinear loads into the grid. Consequently, these nonlinear characteristics induce severe power quality issues, including harmonic distortion, reactive power demands, electromagnetic interference, and overall energy losses [1]–[6]. Within railway

infrastructure, such power quality degradation often causes thermal energy losses in transformers and transmission lines [7]–[10]. Moreover, these disturbances can trigger the malfunction of electrical protection devices [11]–[13], leading to system failures, inflated maintenance costs, and compromised operational safety. Therefore, improving power quality–specifically through harmonic mitigation, current unbalance compensation, and reactive power compensation (power factor (PF) correction)–is imperative for minimizing energy losses and ensuring the stability and reliability of electric railway systems.

Active power filters (APFs) are widely deployed to improve power quality by dynamically detecting and compensating for harmonic currents under fluctuating load conditions. However, APF performance strongly depends on the effectiveness of its control system, particularly the accuracy of reference current calculation, compensating current control, and direct current (DC) bus voltage control. Proportional–integral (PI) controllers are widely used in APF control systems because of their simple structure, ease of implementation, and inherent stability when the closed-loop poles are located in the left half of the complex plane. Despite these advantages, PI controllers require appropriate gain selection to achieve satisfactory dynamic and steady-state performance. Conventional tuning approaches [14]–[18] are generally based on fixed operating conditions. Therefore, optimization-based tuning methods have increasingly been investigated to determine suitable controller parameters and improve harmonic mitigation and overall APF performance [16], [17]. Consequently, determining suitable PI controller parameters remains an important challenge for achieving effective power quality compensation under dynamic railway operating conditions.

In recent years, artificial intelligence (AI) techniques have been increasingly applied to controller-parameter tuning in power-electronic and power-quality applications [19]–[22]. These approaches provide systematic search capabilities for determining controller gains to support optimizing control system performance. Among these, the adaptive Tabu search (ATS) algorithm stands out as a highly efficient metaheuristic technique for identifying optimal controller parameters. ATS is particularly adept at navigating vast solution spaces and adapting to complex, dynamic systems; consequently, it has been successfully implemented across various power electronic domains, including converter design, motor drives, and renewable energy integration. To address the limitations of conventional tuning in railway electrification applications, this study proposes an AI-driven methodology utilizing the ATS algorithm to simultaneously design the compensating current and DC bus voltage PI controllers of an APF. The proposed approach aims to improve harmonic mitigation, current unbalance compensation, and reactive power compensation under severe nonlinear loading. Although recent studies have applied AI-based and metaheuristic optimization to inverter controllers, APF controllers, parameter optimization, and railway power-quality control [19]–[22], the simultaneous optimization of both PI control loops of an APF for railway electrification has received limited attention. Compared with the recent AI-based and metaheuristic optimization approaches reported in [19]–[22], the proposed ATS-based method simultaneously determines four PI gains for the compensating-current and DC-bus voltage controllers using a unified objective function that considers harmonic distortion, current unbalance, and PF.

To validate the proposed control strategy, the Airport Rail Link system in Thailand is utilized as a practical case study. Performance is evaluated through both numerical simulation and real-time hardware-in-the-loop (HIL) implementation, ensuring the validation environment closely mirrors physical hardware conditions. System efficacy is quantified using standard power quality indices–specifically, the percentage of total harmonic distortion of current (%THDi), the percentage of current unbalance factor (%CUF), and PF–in strict accordance with IEEE standards [1]–[3].

The primary contributions of this study are summarized as follows:

- Development of a novel PI controller design methodology for APFs in electric railway systems driven by the ATS algorithm.
- Simultaneous optimization of controller parameters to maximize harmonic mitigation, current unbalance compensation, and PF correction.
- Practical application and modeling of the proposed framework using the Airport Rail Link system in Thailand as a case study.
- Rigorous real-time validation of the proposed control strategy via HIL simulation.
- Comprehensive evaluation of power quality enhancement benchmarked against IEEE standards.

The remainder of this paper is organized as follows. Section 2 details the electric railway system and the APF configuration. Section 3 proposes the mathematical models of the APF control systems. Section 4 outlines the ATS-based PI controller design method. Section 5 presents and analyzes the real-time simulation results. Finally, section 6 concludes the study.

2. ELECTRIC RAILWAY SYSTEM AND ACTIVE POWER FILTER STRUCTURES

Figure 1 illustrates the configuration of the electric railway system under study, detailing the integration of the APF at the traction substation. The system architecture is divided into two primary components: the electric railway network and the APF structure.

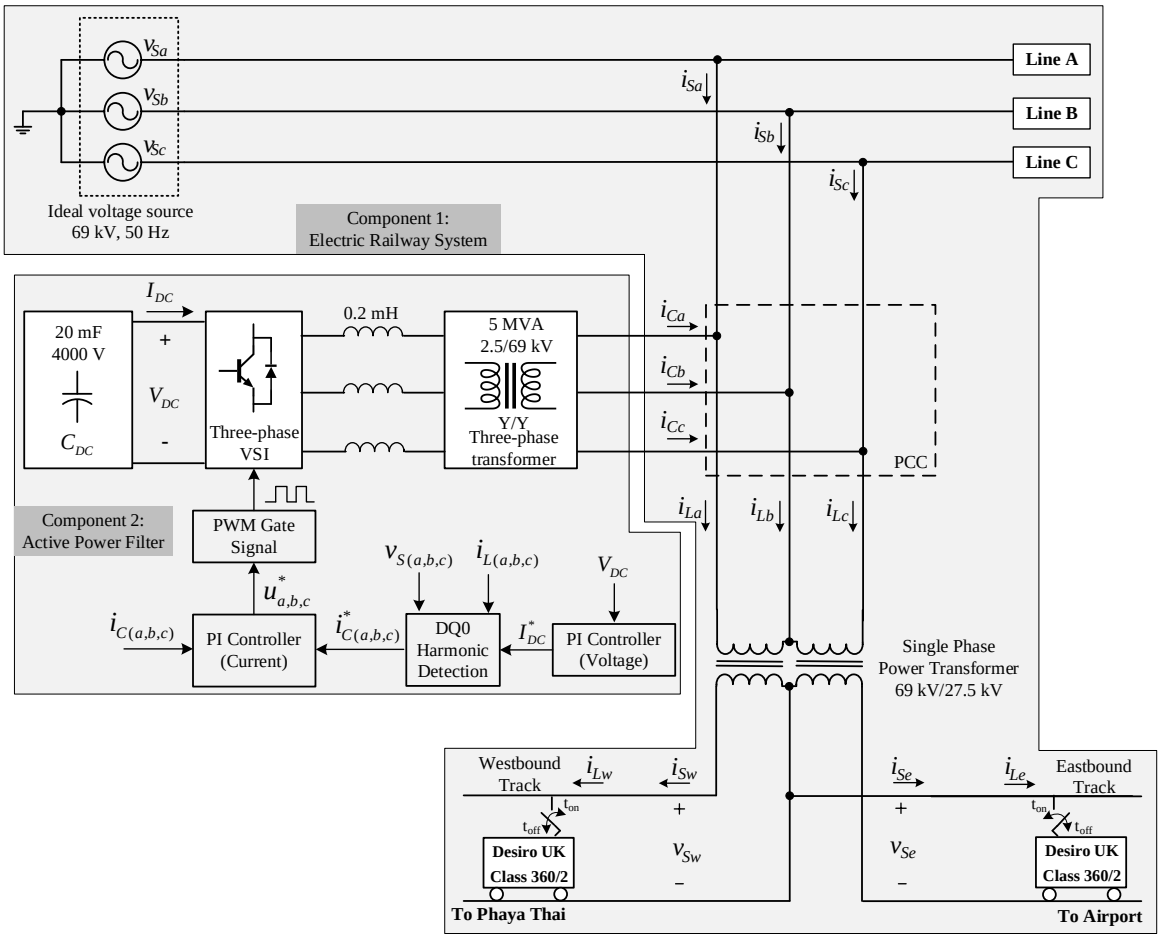


Figure 1. Configuration of the electric railway system with an installed APF

2.1. Structure of the electric railway system

The Airport Rail Link, operational since 2010 [23], serves as a primary transit corridor connecting Suvarnabhumi Airport to central Bangkok (Phaya Thai Station). The network employs a 27.5 kV overhead catenary electrification system. Power is supplied by the Metropolitan Electricity Authority (MEA) via a 69 kV three-phase grid. To accommodate the railway loads, single-phase power transformers connected across phases A-B and B-C step the voltage down from 69 kV to 27.5 kV. This power is subsequently distributed through the overhead lines to two independent single-phase systems powering the eastbound and westbound tracks, as depicted in Figure 1 (Component 1).

The primary dynamic loads on this network are Siemens Desiro UK Class 360/2 electric trains [23], which draw power via pantographs. The onboard electrical subsystems–including power converters, motor speed control systems, three-phase asynchronous traction motors, and auxiliary passenger services–act as severe nonlinear loads. Consequently, these components inject substantial harmonic currents and reactive power back into the grid. Furthermore, the transient nature of train operations causes rapid fluctuations in current demand, complicating conventional harmonic and reactive power compensation efforts. Crucially, the deployment of single-phase transformers across a three-phase supply inherently induces severe phase current unbalance, resulting in significant energy losses in the neutral conductor. To mitigate these multifaceted power quality degradation issues and enhance overall system reliability, an APF is installed in parallel at the point of common coupling (PCC) between the main utility grid and the traction load.

2.2. Structure of the active power filter

While traditionally deployed solely for harmonic current cancellation via the injection of equal but opposite currents, the APF proposed in this study is engineered for multifunctional power quality conditioning. Connected in parallel at the PCC, it is designed to simultaneously execute harmonic mitigation, current unbalance compensation, and reactive power correction. As illustrated in Figure 1 (Component 2), the core hardware architecture of the APF comprises a voltage source inverter (VSI), a DC bus capacitor, interface inductors, and a three-phase coupling transformer. The control architecture relies on a harmonic detection module, a DC bus voltage controller, a compensating current controller, and a pulse-width modulation (PWM) signal generator.

Operationally, the APF initiates power quality conditioning by employing the instantaneous power (PQ) method [24], [25] or synchronous reference frame (DQ0) method [25], [26] to detect harmonics and calculate the precise reference current. In this study, using DQ0 method. A PI controller within the current control loop then governs the VSI output by generating PWM signals. These signals modulate the insulated-gate bipolar transistors (IGBTs) to accurately track the reference current. Concurrently, the DC bus voltage control loop maintains the VSI voltage at a sufficient threshold to guarantee the optimal injection of compensating currents into the PCC. Through this coordinated control strategy, the injected currents effectively neutralize harmonic distortion, balance phase currents, and compensate for reactive power.

3. MATHEMATICAL MODEL OF THE ACTIVE POWER FILTER CONTROL SYSTEMS

The control architecture of the APF comprises a compensating current control loop and a DC bus voltage control loop. In this study, a PI controller is applied to the APF control system. The controller design is grounded in the mathematical models of the plant, as detailed below.

3.1. Compensating current control system

To ensure the compensating current ($i_{C(a,b,c)}$) accurately tracks the reference current ($i^*_{C(a,b,c)}$) generated by the DQ0 harmonic detection algorithm, the PI controller parameters ($K_{P(ic)}, K_{I(ic)}$) must be optimally tuned. The analysis initiates with the differential equation governing the compensating current, expressed as (1):

$$\frac{di_{C(a,b,c)}(t)}{dt} = \frac{v_{inv(a,b,c)}(t)}{aL_C} - \frac{v_{S(a,b,c)}(t)}{a^2 L_C} \tag{1}$$

where a is the winding ratio of a three-phase transformer and $v_{inv(a,b,c)}$ represents the output voltage of the VSI.

Rearranging (1) isolates the dynamic characteristics of the model:

$$v_{inv(a,b,c)}(t) = aL_C \frac{di_{C(a,b,c)}(t)}{dt} + \frac{v_{S(a,b,c)}(t)}{a} \tag{2}$$

Because controlling the derivative term in (2) directly governs $i_{C(a,b,c)}$, the plant of the compensating current control system is modeled by the term "$aL_C \frac{di_{C(a,b,c)}}{dt}$." The control signal ($u^*_{a,b,c}$) dictates the PWM switching states for the IGBTs within the VSI. The closed-loop control diagram for this current control loop in the s-domain (Laplace transform) is illustrated in Figure 2.

From Figure 2, the closed-loop transfer function of the compensating current control with a PI controller can be considered as shown in (3):

$$\frac{I_{C(a,b,c)}(s)}{I^*_{C(a,b,c)}(s)} = \frac{\frac{1}{aL_C}\left(K_{P(ic)}s + K_{I(ic)}\right)}{s^2 + \left(\frac{K_{P(ic)}}{aL_C}\right)s + \frac{K_{I(ic)}}{aL_C}} \tag{3}$$

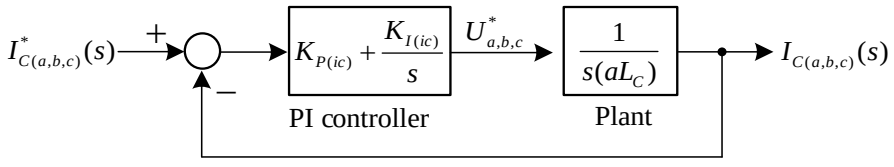


Figure 2. Closed-loop control diagram of the compensating current control system

3.2. Direct current bus voltage control system

Maintaining the DC bus voltage (V_{DC}) at a constant reference value (4000 V) is critical, as fluctuations directly compromise the magnitude and operational direction of the compensating current. This study employs an indirect DC bus voltage control strategy utilizing a PI controller integrated with the DQ0 harmonic detection method. The tuning of the PI parameters ($K_{P(VDC)}, K_{I(VDC)}$) relies on the differential equation of the DC bus voltage, as presented in (4).

$$i_{DC} = C_{DC}\frac{dv_{DC}}{dt} \tag{4}$$

The plant of the DC bus voltage control loop is defined as "$C_{DC}\frac{dv_{DC}}{dt}$", where i_{DC} feeds into the DQ0 harmonic detection method to influence the active power exchange. Applying the Laplace transform yields the closed-loop s-domain block diagram illustrated in Figure 3. Based on this control architecture, the closed-loop transfer function of the DC bus voltage regulation is formulated as shown in (5):

$$\frac{V_{DC}(s)}{V_{DC}^{*}} = \frac{\frac{1}{C_{DC}}\left(K_{P(VDC)}s + K_{I(VDC)}\right)}{s^2 + \frac{K_{P(VDC)}}{C_{DC}}s + \frac{K_{I(VDC)}}{C_{DC}}} \tag{5}$$

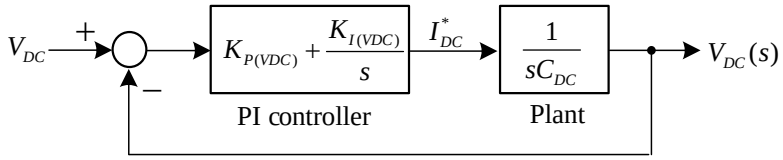


Figure 3. Closed-loop control diagram of the DC bus voltage control system

4. ARTIFICIAL INTELLIGENCE METHOD USING ADAPTIVE TABU SEARCH

The ATS is an advanced AI-based metaheuristic algorithm designed to systematically identify optimal system parameters. Evolving from the foundational Tabu search (TS) algorithm [27], ATS introduces two critical enhancement mechanisms to overcome standard search limitation: backtracking and an adaptive search radius [28], [29]. TS-based and other metaheuristic algorithms have also been applied to optimize control parameters in power electronic converters [30], motor drives [31], and APFs [32]. As illustrated in Figure 4, the backtracking mechanism permits the algorithm to revisit previously explored regions of the solution space, thereby preventing entrapment in local optima and facilitating the discovery of superior global solutions. Concurrently, the adaptive search radius mechanism iteratively reduces the search boundary as the optimization process advances, effectively concentrating the computational effort near the most promising solution. This dynamic radius adjustment is mathematically expressed as shown in (6):

$$radius_{\text{new}} = \frac{radius_{\text{old}}}{DF} \tag{6}$$

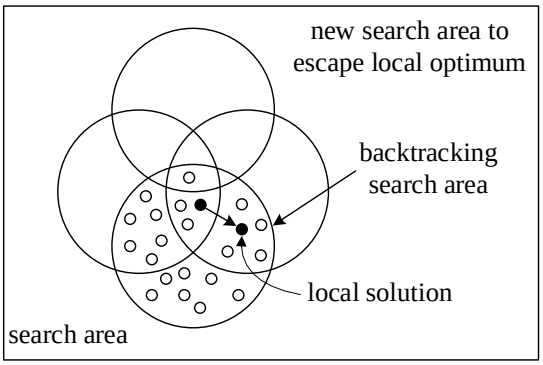


Figure 4. Backtracking mechanism

The successful deployment of the ATS algorithm requires the formulation of a robust objective function tailored to the specific operational goal of the system. In this study, ATS is utilized to precisely tune the PI controller parameters ($K_{P(ic)}, K_{I(ic)}, K_{P(VDC)}, K_{I(VDC)}$) within the APF control architecture to maximize power quality improvement across the electric railway system. The search boundary for $K_{P(ic)}, K_{I(ic)}, K_{P(VDC)}$, and $K_{I(VDC)}$ parameters are strictly bounded by classical control stability criteria, ensuring that all closed-loop poles remain securely located in the left half of the complex plane [26], [33]. Furthermore, the objective function is explicitly formulated to quantify the APF's efficacy in mitigating specific grid disturbances. Consequently, key power quality indices–derived in strict accordance with IEEE standards–are integrated into the objective function, as defined in (7):

$$J = w_1|\%\text{THDi}^* - \%\text{THDi}| + w_2|\%\text{CUF}^* - \%\text{CUF}| + w_3|\text{PF}^* - \text{PF}| \quad (7)$$

where $\%\text{THDi}^*$ represents the acceptable %THDi, $\%\text{CUF}^*$denotes the acceptable %CUF, PF is the acceptable PF, and w_1, w_2, and w_3 are the weighting factors.

5. REAL-TIME HARDWARE-IN-THE-LOOP SIMULATION RESULTS AND DISCUSSION

The validation of this study is conducted using a real-time HIL simulation technique. This approach provides a cost-effective and flexible framework for validating engineering systems. Moreover, it enables the investigation of large-scale systems that cannot be physically realized in laboratory environments using conventional tools and embedded control hardware. Recent studies have demonstrated the effectiveness of real-time and controller HIL platforms for evaluating APF control strategies and harmonic mitigation performance [34], [35]. The real-time HIL configuration, results, and discussion are presented as follows:

5.1. Hardware-in-the-loop configuration

HIL simulation is a standard paradigm for the real-time validation of power electronic control systems, enabling the execution of complex plant models with high fidelity and deterministic timing. In this study, the plant–comprising the electric railway system, the transient traction load, and the APF power topology–is modeled entirely within MATLAB/Simulink. Conversely, the APF control architecture, which encompasses the DQ0 harmonic detection algorithm and the ATS-optimized PI controllers for compensating current and DC bus voltage regulation, is physically deployed on an eZdsp F28335 digital signal processor (DSP). As depicted in Figure 5, the real-time simulator facilitates continuous, bidirectional signal exchange between the MATLAB/Simulink plant model and the external eZdsp hardware.

In Figure 5, the HIL setup consists of a host computer running MATLAB/Simulink, an eZdsp F28335 DSP board, Code Composer Studio, and a USB joint test action group (JTAG) emulator for program downloading and communication. The controller operates at a sampling frequency of 100 kHz. At each sampling instant, the source voltages, load currents, compensating currents, and DC-bus voltage measured from the MATLAB/Simulink plant model are sent to the eZdsp F28335. The DSP then executes the DQ0 harmonic detection algorithm, calculates the reference compensating currents, performs the DC-bus voltage and compensating-current PI control, and generates the PWM signals. These signals are returned to the MATLAB/Simulink APF model to control the VSI in the next simulation step. This closed-loop signal exchange is continuously repeated throughout the HIL simulation to evaluate the proposed controller under dynamic operating conditions of the electric railway system.

5.2. Optimization of proportional–integral controller parameters via adaptive Tabu search

The ATS algorithm's parameter search is strictly constrained by the dual requirements of minimizing the objective function and closed-loop stability preservation. The optimization thresholds are established in strict accordance with IEEE standards; thus, the target constraints are defined as $\%\text{THDi}^* = 3\%$, $\%\text{CUF}^* = 2\%$, and $\text{PF}^* = 0.9$. The weighting factors were selected according to the control priorities of the APF. Since harmonic current mitigation is the primary objective of the proposed APF, a higher weight of $w_1 = 0.6$ is assigned to %THDi. Meanwhile, $w_2 = 0.2$ and $w_3 = 0.2$ are assigned to %CUF and PF, respectively, so that current unbalance reduction and PF correction are also considered in the optimization. The ATS parameters used in the optimization were selected through preliminary trial-and-error tests. The initial search radius was set to 1.5, the decreasing factor (DF) was 1.1, the initial number of neighboring solutions was 40, and the number of neighboring solutions during the search was 50. The ATS searches for four PI-controller parameters, namely $K_{P(ic)}$, $K_{I(ic)}$, $K_{P(VDC)}$, and $K_{I(VDC)}$. At each search round, candidate parameter sets are evaluated using the objective function in (7), and the solution providing the lowest objective-function value while satisfying the stability constraints is retained. The adaptive search radius and backtracking mechanisms are then applied to continue the search. The optimization process is

terminated when no further meaningful improvement in the objective-function value is observed or when the maximum number of search rounds is reached.

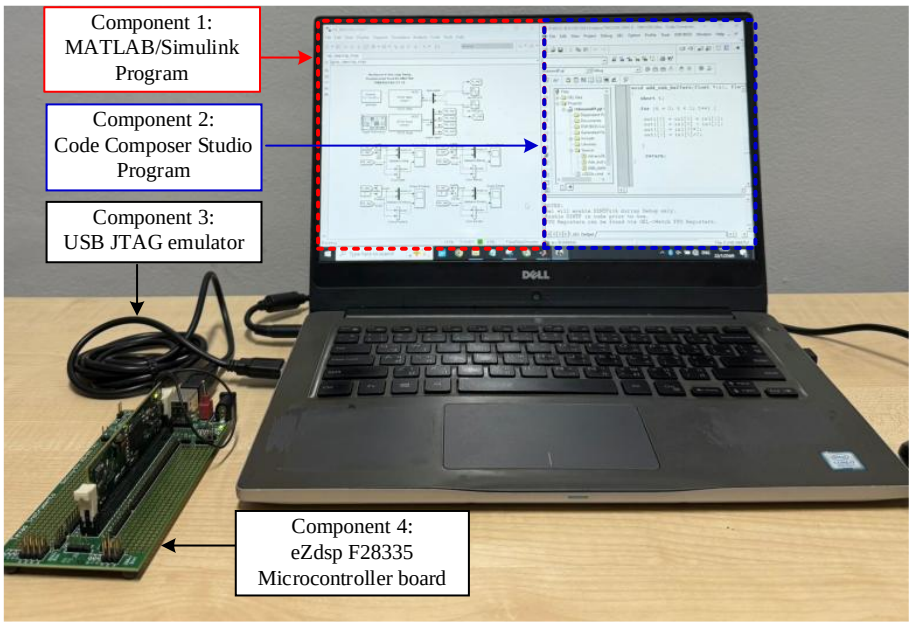


Figure 5. Real-time HIL simulation setup interface between MATLAB/Simulink and the eZdsp F28335

As illustrated by the convergence curve in Figure 6, the objective function exhibits a stepwise reduction rather than a smooth monotonic descent. This behavior indicates that the ATS algorithm iteratively transitions between locally improved feasible regions, followed by solution refinement within each region. A significant decrease in the objective value is observed during the early iterations, suggesting that the APF performance is highly sensitive to PI gain selection and that conventional tuning approaches may become trapped in suboptimal regions. After approximately 25 iterations, the objective function reaches a steady plateau with negligible variation, indicating that the optimal solution within the defined search space has been attained and that further iterations provide only marginal improvement. These convergence characteristics demonstrate both the rapid search capability and the robustness of the ATS algorithm in maintaining feasible and stable solutions under multi-objective power quality constraints.

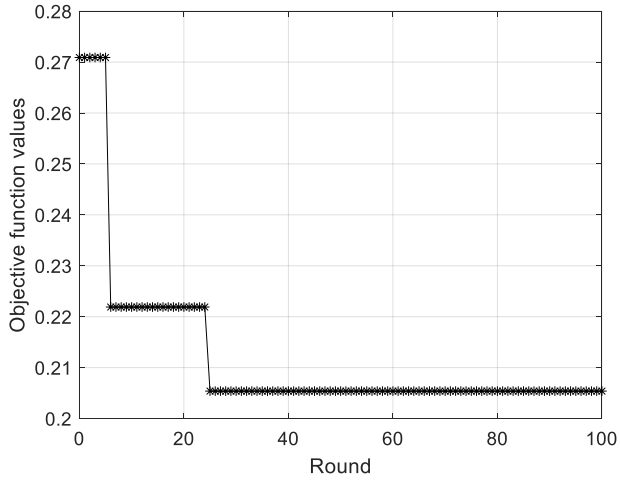


Figure 6. Convergence of the objective function during ATS-based PI controller parameter optimization

This result confirms that the ATS optimization successfully identified the global minimum of the objective function at optimal PI gains of $K_{P(ic)} = 138.95, K_{I(ic)} = 1.48 \times 10^6, K_{P(VDC)} = 9.04,$ and $K_{I(VDC)} = 1962.28$. These finalized parameters are subsequently embedded into the HIL APF control system to execute power quality conditioning. The ATS optimization was performed offline before implementation of the optimized PI gains in the real-time APF controller. Therefore, the ATS search does not impose an additional online computational burden on the eZdsp F28335 during APF operation.

5.3. Evaluation of the power quality improvements

The dynamic performance of the ATS-optimized APF in mitigating power quality disturbances is rigorously evaluated. Prior to compensation, the railway system exhibits severe harmonic distortion, unbalance current, and low PF. However, upon the activation of the APF and the subsequent injection of compensating currents at the PCC at 0.1 s, the source currents (i_{Sa}, i_{Sb}, i_{Sc}) rapidly transition to balanced, sinusoidal waveforms. As illustrated in Figure 7, this transient response signifies a substantial restoration of power quality compared to the uncompensated state. Furthermore, the steady-state power quality indices successfully comply with IEEE standard limits, as detailed in Figures 8 and 9. To benchmark the efficacy of the proposed method, the results are compared with the conventional PI tuning method.

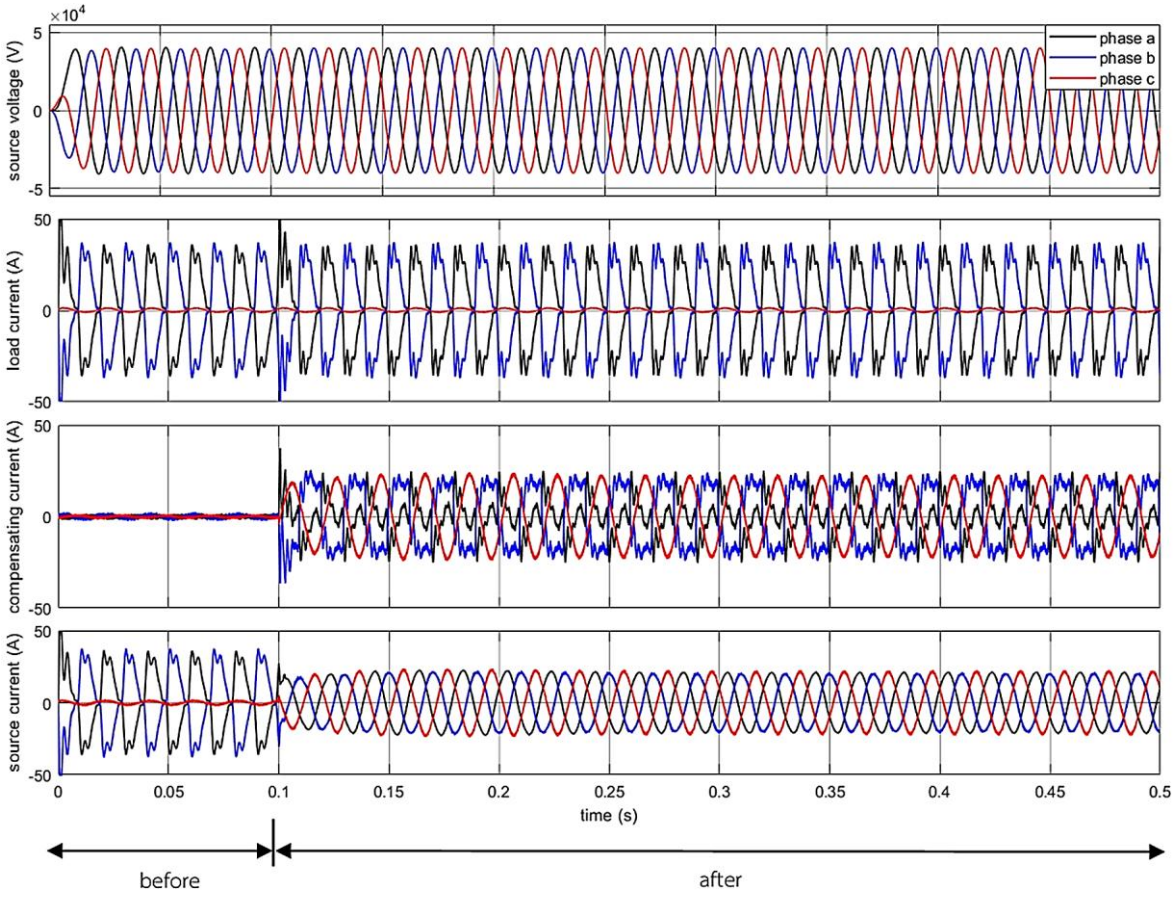


Figure 7. Real-time HIL results of the electric railway system before and after APF compensation

Table 1 provides a quantitative comparison of power quality performance indices before and after compensation, highlighting the effectiveness of the proposed ATS-based PI tuning method relative to the conventional design approach. Prior to compensation, the system exhibits severe power quality degradation, with %THDi values of 25.62%, 24.68%, and 1.44% for phases a, b, and c, respectively, along with a critically high %CUF of 99.83% and a low PF of 0.67. These values significantly violate IEEE standard limits, confirming the highly distorted and unbalanced operating condition of the electric railway system.

Table 1. Comparison of power quality indices before and after APF compensation

Performance indices	%THDia	%THDib	%THDic	%CUF	PF
IEEE standards limit	Less than 5%	Less than 5%	Less than 5%	Less than 3%	More than 0.85
Before compensation (0<t<0.1 s.)	25.62%	24.68%	1.44%	99.83%	0.67
	Does not comply	Does not comply	Does not comply	Does not comply	Does not comply
After compensation (t>0.1 s.)					
- Conventional design method [17]	4.08%	5.19%	4.83%	3.75%	0.92
	Complies	Does not comply	Complies	Does not comply	Complies
- ATS design method (proposed)	2.89%	3.17%	3.02%	2.30%	0.97
	Complies	Complies	Complies	Complies	Complies

* Evaluation using IEEE standard limits [1]–[3]

After compensation using the conventional PI tuning method based on [17], partial improvement is observed. The %THDi values are reduced to 4.08%, 5.19%, and 4.83%, respectively. Although phases a and c satisfy the IEEE limit of 5%, phase b still exceeds the allowable threshold. Similarly, the %CUF remains at 3.75%, which is above the 3% limit, indicating that the conventional tuning approach is insufficient to fully mitigate current unbalance. The PF is improved to 0.92, which meets the standard requirement; however, the overall performance remains suboptimal due to incomplete harmonic and unbalance compensation.

In contrast, the proposed ATS-based method achieves improved harmonic mitigation for all three source current phases. As shown in Figure 8(a), the %THDi of the phase a source current is reduced to 2.89%. Figure 8(b) shows that the %THDi of the phase b source current is reduced to 3.17%, while Figure 8(c) shows a %THDi of 3.02% for the phase c source current. Compared to the conventional method, the ATS approach achieves additional reductions of approximately 29.2%, 38.9%, and 37.5% in %THDi for phases a, b, and c, respectively. Moreover, the %CUF is significantly decreased from 3.75% to 2.30%, representing an improvement of approximately 38.7%. The PF is further enhanced from 0.92 to 0.97, indicating improved reactive power compensation and overall system efficiency.

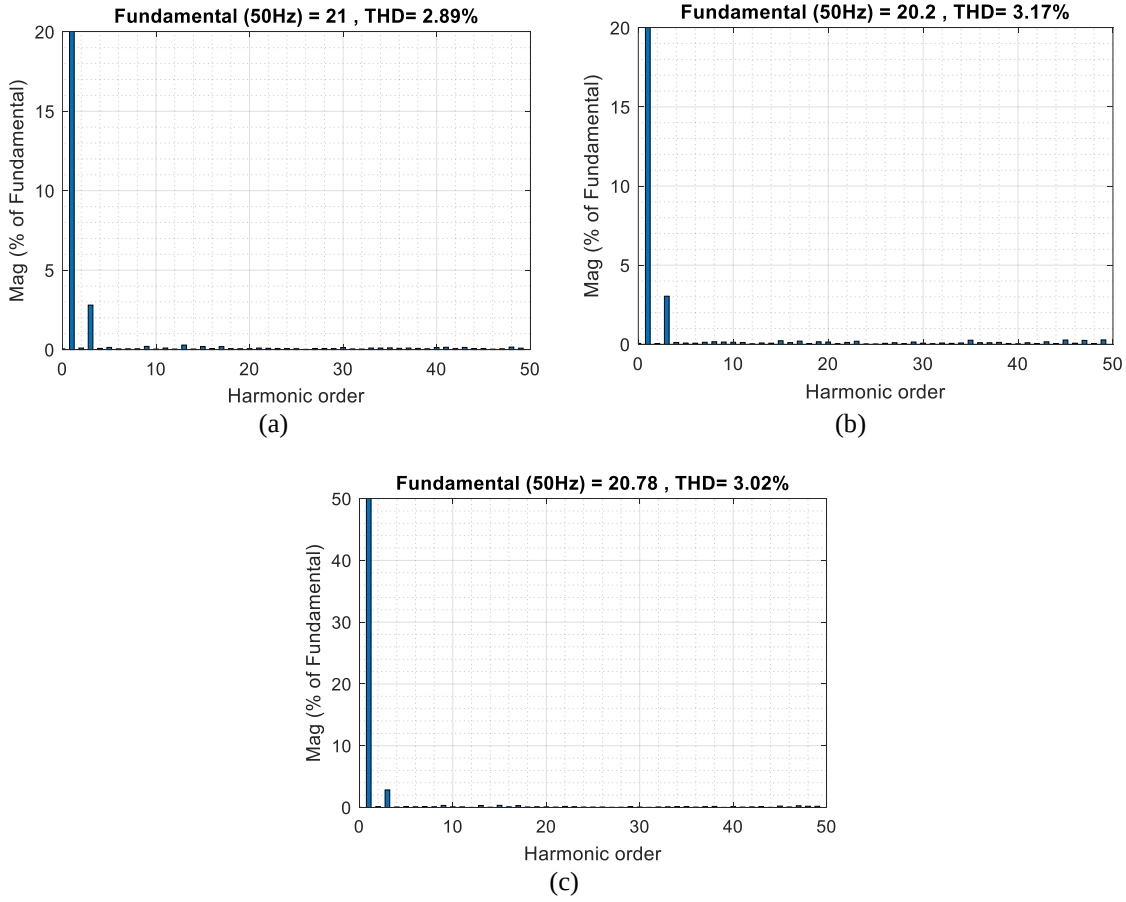


Figure 8. Harmonic spectrum of the source currents after APF compensation; (a) phase a, (b) phase b, and (c) phase c

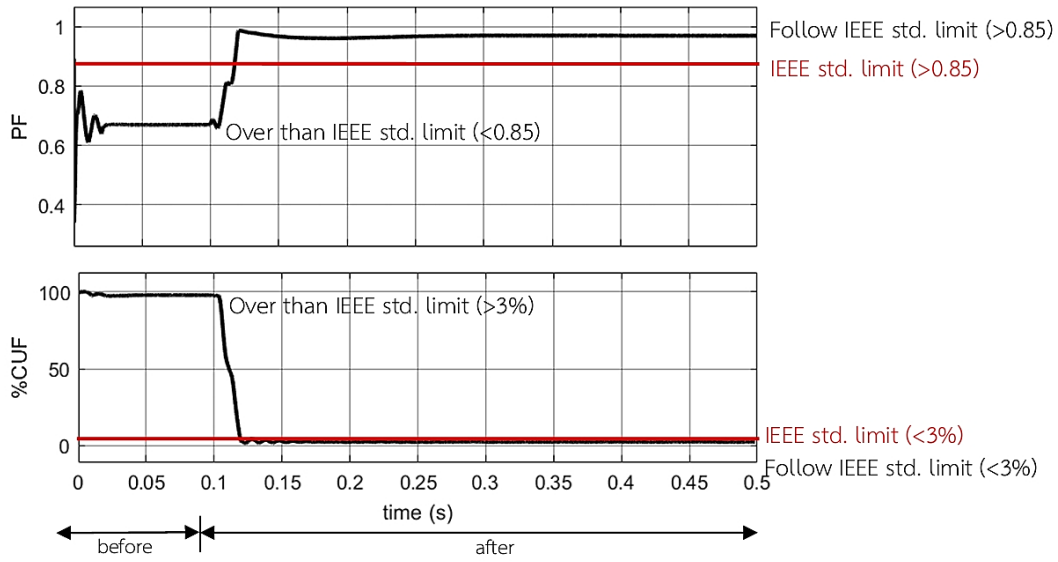


Figure 9. Real-time HIL results of PF correction and current unbalance compensation

The superior performance of the ATS-based design can be attributed to its systematic search for the four PI-controller parameters under the defined multi-objective constraints. Unlike conventional tuning methods, which typically rely on fixed tuning rules, heuristic adjustments, or trial-and-error procedures, the ATS algorithm evaluates multiple candidates gain combinations according to the objective function in (7). The backtracking mechanism allows the search to move away from less promising regions, while the adaptive search radius provides a broader exploration during the early search stage and progressively refines the search around better solutions. In addition, the simultaneous tuning of the compensating current and DC-bus voltage PI controllers allows the two control loops to be coordinated rather than adjusted independently. The weighted objective function gives higher priority to harmonic mitigation while still considering current-unbalance reduction and PF correction. As a result, the optimized PI gains provide a better overall balance among the three power-quality objectives, which is reflected in the lower %THDi and %CUF and the higher PF compared with the conventional PI design in Table 1. However, the proposed approach requires an offline optimization stage, which introduces additional computational effort during the controller-design phase. Furthermore, its performance depends on the appropriate selection of weighting factors in the objective function, which may require expert knowledge or further sensitivity analysis. Future work may focus on adaptive or self-tuning weighting strategies to further improve the control performance.

6. CONCLUSION

This study presents a novel AI-driven method for the optimal design of PI controllers within APFs deployed in electric railway system. Specifically, the ATS algorithm was successfully implemented to systematically tune the PI parameters, aiming to maximize power quality enhancements across highly nonlinear traction loads. The proposed control architecture was rigorously evaluated utilizing the electrical infrastructure of the Airport Rail Link system in Thailand through real-time HIL simulation. Empirical results definitively confirmed that the ATS-optimized APF significantly outperforms conventional tuning techniques, achieving superior harmonic mitigation, current unbalance compensation, and PF correction that strictly comply with IEEE standard limits. Ultimately, this research provides a robust, systematic framework for APF controller design. By bridging advanced AI optimization with practical real-time implementation, this study offers a highly effective and scalable strategy for ensuring grid stability, reliability, and energy efficiency in modern electric railway infrastructure.

ACKNOWLEDGMENTS

The authors acknowledge King Mongkut's University of Technology North Bangkok and Rajamangala University of Technology Suvarnabhumi for providing facilities and resources that supported this research.

FUNDING INFORMATION

This research was supported by Rajamangala University of Technology Suvarnabhumi, Thailand Science Research and Innovation (TSRI), and the National Science, Research and Innovation Fund (NSRF) under Research Grant No. FRB690024/0173-16.

AUTHOR CONTRIBUTIONS STATEMENT

This journal uses the Contributor Roles Taxonomy (CRediT) to recognize individual author contributions, reduce authorship disputes, and facilitate collaboration.

Name of Author	C	M	So	Va	Fo	I	R	D	O	E	Vi	Su	P	Fu
Chakrit Panpean	✓	✓	✓	✓	✓	✓	✓	✓	✓		✓			✓
Chirdpong Deelertpaiboon		✓	✓	✓	✓	✓			✓					
Jeerawan Homjan	✓	✓	✓	✓	✓	✓			✓		✓		✓	✓
Ittiphong Yongyee						✓	✓	✓		✓		✓	✓	✓
Warunee Srisongkram						✓	✓	✓		✓		✓		✓
Napat Watjanatepin						✓	✓			✓		✓		

C : **C**onceptualization
M : **M**ethodology
So : **So**ftware
Va : **Va**lidation
Fo : **Fo**rmal analysis
I : **I**nvestigation
R : **R**esources
D : **D**ata Curation
O : Writing - **O**riginal Draft
E : Writing - Review & **E**diting
Vi : **Vi**sualization
Su : **Su**pervision
P : **P**roject administration
Fu : **Fu**nding acquisition

CONFLICT OF INTEREST STATEMENT

Authors state no conflict of interest.

DATA AVAILABILITY

Derived data supporting the findings of this study are available from the corresponding author [IY] or the first author [CP] on request.

REFERENCES

[1] "IEEE Standard Definitions for the Measurement of Electric Power Quantities Under Sinusoidal, Nonsinusoidal, Balanced, or Unbalanced Conditions," *IEEE Std 1459-2025* (Revision of IEEE Std 1459-2010), pp. 1–61, May 2025, doi: 10.1109/IEEESTD.2025.11004570.

[2] "IEEE Recommended Practice for Monitoring Electric Power Quality," *IEEE Std 1159-2019* (Revision of IEEE Std 1159-2009), pp. 1–98, Aug. 2019, doi: 10.1109/IEEESTD.2019.8796486.

[3] "IEEE Standard for Harmonic Control in Electric Power Systems," *IEEE Std 519-2022 (Revision of IEEE Std 519-2014)*, pp. 1–31, Aug. 2022, doi: 10.1109/IEEESTD.2022.9848440.

[4] "Electromagnetic compatibility (EMC)—Part 3-2: Limits—Limits for harmonic current emissions (equipment input current ≤16 A per phase)," *IEC 61000-3-2:2018+AMD1:2020+AMD2:2024 CSV*, International Electrotechnical Commission (IEC), 2024.

[5] "Voltage characteristics of electricity supplied by public electricity networks," *EN 50160:2022*, European Committee for Electrotechnical Standardization (CENELEC), 2022.

[6] "Harmonic Regulation for Business and Industrial Use," *PRC-PQG-01/2011*, Metropolitan Electricity Authority (MEA), Bangkok, Thailand, 2011.

[7] S. M. M. Gazafrudi, A. T. Langerudy, E. F. Fuchs, and K. Al-Haddad, "Power quality issues in railway electrification: A comprehensive perspective," *IEEE Trans. Ind. Electron.*, vol. 62, no. 5, pp. 3081–3090, May 2015, doi: 10.1109/TIE.2014.2386794.

[8] C. A. Charalambous, A. Demetriou, A. L. Lazari, and A. I. Nikolaidis, "Effects of electromagnetic interference on underground pipelines caused by the operation of high voltage AC traction systems: The impact of harmonics," *IEEE Trans. Power Del.*, vol. 33, no. 6, pp. 2664–2672, Dec. 2018, doi: 10.1109/TPWRD.2018.2803080.

[9] W. Song, J. Fang, Z. Jiang, M. Staines, and R. Badcock, "AC loss effect of high-order harmonic currents in a single-phase 6.5 MVA HTS traction transformer," *IEEE Trans. Appl. Supercond.*, vol. 29, no. 5, pp. 1–5, Aug. 2019, doi: 10.1109/TASC.2019.2901014.

[10] H. Hu *et al.*, "Traction power systems for electrified railways: Evolution, state of the art, and future trends," *Railway Eng. Sci.*, vol. 32, no. 1, pp. 1–19, Mar. 2024, doi: 10.1007/s40534-023-00320-6.

[11] H. Farzin, M. Monadi, M. Fotuhi-Firuzabad, and M. Savaghebi, "A reliability model for overcurrent relays considering harmonic-related malfunctions," *Int. J. Electr. Power Energy Syst.*, vol. 131, Oct. 2021, Art. no. 107093, doi: 10.1016/j.ijepes.2021.107093.

[12] Z. M. Ali, M. Ćalasan, F. Jurado, and S. H. E. A. Aleem, "Complexities of power quality and harmonic-induced overheating in modern power grids studies: Challenges and solutions," *IEEE Access*, vol. 12, pp. 151554–151597, 2024, doi:

10.1109/ACCESS.2024.3477729.
[13] I. A. Metwally, "Failures, monitoring and new trends of power transformers," *IEEE Potentials*, vol. 30, no. 3, pp. 36–43, May 2011, doi: 10.1109/MPOT.2011.940233.
[14] R. Errouissi and A. Al-Durra, "Design of PI controller together with active damping for grid-tied LCL-filter systems using disturbance-observer-based control approach," *IEEE Trans. Ind. Appl.*, vol. 54, no. 4, pp. 3820–3831, Jul./Aug. 2018, doi: 10.1109/TIA.2018.2823258.
[15] K. Kołek and A. Firlit, "A new optimal current controller for a three-phase shunt active power filter based on Karush–Kuhn–Tucker conditions," *Energies*, vol. 14, no. 19, Oct. 2021, Art. no. 6381, doi: 10.3390/en14196381.
[16] M. L. Duc, L. Hlavaty, P. Bilik, and R. Martinek, "Harmonic mitigation using meta-heuristic optimization for shunt adaptive power filters: A review," *Energies*, vol. 16, no. 10, May 2023, Art. no. 3998, doi: 10.3390/en16103998.
[17] C. Panpean, N. Mangkhala, and K.-L. Areerak, "The harmonic mitigation for heavy rail systems using shunt active power filter," in *Proc. 12th Int. Elect. Eng. Congr. (iEECON)*, Mar. 2024, pp. 1–6, doi: 10.1109/ieecon60677.2024.10537974.
[18] A. Tamer, L. Zellouma, M. T. Benchouia, and A. Krama, "Adaptive linear neuron control of three-phase shunt active power filter with anti-windup PI controller optimized by particle swarm optimization," *Comput. Electr. Eng.*, vol. 96, Dec. 2021, Art. no. 107471, doi: 10.1016/j.compeleceng.2021.107471.
[19] M. A. Ebrahim, B. A. Aziz, M. N. F. Nashed, and F. A. Osman, "Optimal design of controllers and harmonic compensators for three-level cascaded control in stationary reference frame for grid-supporting inverters-based AC microgrid," *Energy Rep.*, vol. 8, pp. 860–877, Nov. 2022, doi: 10.1016/j.egyr.2021.11.248.
[20] A. Umadevi, L. Lakshminarasimman, and A. Sakthivel, "Optimal design of shunt active power filter for mitigation of interharmonics in grid tied photovoltaic system," *Electr. Power Syst. Res.*, vol. 220, Jul. 2023, Art. no. 109232, doi: 10.1016/j.epsr.2023.109232.
[21] B. Amini, H. Rastegar, and M. Pichan, "An optimized proportional resonant current controller based genetic algorithm for enhancing shunt active power filter performance," *Int. J. Electr. Power Energy Syst.*, vol. 156, Feb. 2024, Art. no. 109738, doi: 10.1016/j.ijepes.2023.109738.
[22] D. K. Nishad, A. N. Tiwari, S. Khalid, S. Gupta, and A. Shukla, "AI based UPQC control technique for power quality optimization of railway transportation systems," *Sci. Rep.*, vol. 14, no. 1, Aug. 2024, Art. no. 17935, doi: 10.1038/s41598-024-68575-5.
[23] Department of Rail Transport, Ministry of Transport, Thailand, "Railway electrification system," 2020. [Online]. Available: https://www.drt.go.th/library
[24] H. Akagi, E. H. Watanabe, and M. Aredes, *Instantaneous Power Theory and Applications to Power Conditioning*, 2nd ed. Hoboken, NJ, USA: Wiley-IEEE Press, 2017, doi: 10.1002/9781119307181.
[25] P. Santiprapan, K.-L. Areerak, and K.-N. Areerak, "A novel harmonic identification algorithm for the active power filters in non-ideal voltage source systems," *J. Power Electron.*, vol. 17, no. 6, pp. 1637–1649, Nov. 2017, doi: 10.6113/JPE.2017.17.6.1637.
[26] P. Santiprapan, K.-L. Areerak, and K.-N. Areerak, "An adaptive gain of proportional-resonant controller for an active power filter," *IEEE Trans. Power Electron.*, vol. 39, no. 1, pp. 1433–1446, Jan. 2024, doi: 10.1109/TPEL.2023.3319476.
[27] F. Glover and M. Laguna, *Tabu Search*. New York, NY, USA: Springer, 1997, doi: 10.1007/978-1-4615-6089-0.
[28] S. Sujitjorn, T. Kulworawanichpong, D. Puangdownreong, and K.-N. Areerak, "Adaptive tabu search and applications in engineering design," *Integrated Intelligent Systems for Engineering Design*, The Netherlands: IOS Press, 2006, pp. 233–257.
[29] J. Pakdeeto, S. Wansungnoen, K.-N. Areerak, and K.-L. Areerak, "Optimal speed controller design of commercial BLDC motor by adaptive tabu search algorithm," *IEEE Access*, vol. 11, pp. 79710–79720, 2023, doi: 10.1109/ACCESS.2023.3300233.
[30] B. Li *et al.*, "Current harmonic suppression for GaN totem-pole PFC converter based on adaptive active damping with tabu search algorithm," *IEEE Trans. Power Electron.*, vol. 41, no. 6, pp. 9180–9193, Jun. 2026, doi: 10.1109/TPEL.2026.3653474.
[31] Y. Cao, G. Wang, J. Li, D. Yan, and T. Shi, "A self-optimization commutation correction strategy integrating model calculation and tabu search for high-speed BLDCM," *IEEE Trans. Power Electron.*, vol. 40, no. 4, pp. 5700–5714, Apr. 2025, doi: 10.1109/TPEL.2024.3501301.
[32] R. Kumar, H. O. Bansal, A. R. Gautam, O. P. Mahela, and B. Khan, "Experimental investigations on particle swarm optimization based control algorithm for shunt active power filter to enhance electric power quality," *IEEE Access*, vol. 10, pp. 54878–54890, 2022, doi: 10.1109/ACCESS.2022.3176732.
[33] G. F. Franklin, J. D. Powell, and A. Emami-Naeini, *Feedback Control of Dynamic Systems*, 8th ed. Harlow, U.K.: Pearson, 2019, pp. 614–655.
[34] N. F. Guerrero-Rodríguez *et al.*, "Modelling real non-linear loads for a controller hardware-in-the-loop configuration to evaluate a shunt active power filter," *Energy Rep.*, vol. 12, pp. 1947–1976, Dec. 2024, doi: 10.1016/j.egyr.2024.07.056.
[35] S. Sharma, V. Verma, and R. K. Behera, "Real-time implementation of shunt active power filter with reduced sensors," *IEEE Trans. Ind. Appl.*, vol. 56, no. 2, pp. 1850–1861, Mar./Apr. 2020, doi: 10.1109/TIA.2019.2957734.

BIOGRAPHIES OF AUTHORS



Chakrit Panpean received the B.Eng. (Hons.), M.Eng., and Ph.D. degrees in electrical engineering from Suranaree University of Technology (SUT), Thailand, in 2015, 2017, and 2021, respectively. From June 2019 to December 2019, he was a visiting student conducting short-term research at the Institute for Aerospace Technology (IAT), University of Nottingham, Nottingham, U.K. In 2022, he was a lecturer in the School of Electrical Engineering, Rajamangala University of Technology Isan (RMUTI), Thailand. Since 2023, he has been a lecturer in the Department of Instrumentation and Electronics Engineering, Faculty of Engineering, King Mongkut's University of Technology North Bangkok (KMUTNB), Thailand. He received the title of assistant professor of electrical engineering in 2024. His main research interests include power quality improvement, motor drive, electric railway systems, and AI applications. He can be contacted at email: chakrit.p@eng.kmutnb.ac.th.



Chirdpong Deelertpaiboon received his B.Eng. and M.Eng. degrees in electrical engineering from the University of Wisconsin-Madison, USA, and his D.Eng. in Mechatronics from the Asian Institute of Technology, Thailand. He has been with King Mongkut's University of Technology North Bangkok since 2009, where he currently serves as an assistant professor and head of the Department of Instrumentation and Electrical Energy Engineering. His research lies in control systems, applied mechatronics, machine learning, and robotics. He has published widely on autonomous navigation, quadruped robot control and fuzzy logic applications, and has been actively involved in developing medical robotics. He can be contacted at email: chirdpong.d@eng.kmutnb.ac.th.



Jeerawan Homjan received her B.Eng. and M.Eng. degrees in electrical engineering from Suranaree University of Technology (SUT), Thailand, in 2015 and 2019, respectively. In 2020, she was a lecturer in the Department of Mechatronics Engineering, Thaksin University, Phatthalung Campus, Thailand. In 2020, she was a lecturer in the School of Mechatronics Engineering, Institute of Engineering, Suranaree University of Technology, Thailand. Since 2022, she has been a lecturer in the Department of Mechatronics Engineering, Faculty of Engineering and Architecture, Rajamangala University of Technology Suvarnabhumi (RMUTSB), Thailand, and since 2024, she has been an assistant professor in electrical engineering. Her main research interests include power electronics, control systems, motor drives, energy saving, artificial intelligence, intelligent applications, electric vehicles, and LED solar simulators. She can be contacted at email: jeerawan.h@rmutsb.ac.th.



Ittiphong Yongyee received B.S.Ind.Ed. degree from King Mongkut's Institute of Technology Ladkrabang, Thailand, in 2016, M.Eng. degree from King Mongkut's University of Technology North Bangkok, in 2018, and Ph.D. degree from King Mongkut's University of Technology North Bangkok, in 2024. Since 2022, he has been a lecturer in the Department of Mechatronics Engineering, Faculty of Engineering and Architecture, Rajamangala University of Technology Suvarnabhumi (RMUTSB), Thailand, and since 2025, he has been an assistant professor in electrical engineering. His research interests are high voltage equipment, automation systems, intelligent control system, and robotics. He can be contacted at email: ittiphong.y@rmutsb.ac.th.



Warunee Srisongkram received her B.Eng. degree from Rajamangala Institute of Technology, Thailand in 1996, M.Sc. degree from King Mongkut's University of Technology North Bangkok in 2001, M.Eng. degree from Rajamangala University of Technology Thanyaburi in 2008, and D.Eng. degree at the Sirindhorn International Thai-German Graduate School of Engineering, King Mongkut's University of Technology North Bangkok, Bangkok, Thailand. She is currently an assistant professor in the Department of Electrical Engineering at Rajamangala University of Technology Suvarnabhumi (RMUTSB), Thailand. Her research interests are automation controllers, renewable energy, and also the electrical stress investigation and insulation coordination of HV equipment in substations. She can be contacted at email: warunee.s@rmutsb.ac.th.



Napat Watjanatepin earned a B.S.Tech.Ed. (Electrical Engineering) degree from Thailand's Institute of Technology Vocational Education in 1985 and an M.S.Tech.Ed. (Electrical Technology) degree from King Mongkut's Institute of Technology North Bangkok in 1991. Power electronics and drives, renewable energy, photovoltaic energy system, LED solar simulators, LED for horticulture, and engineering education are among his research interests. He won a gold medal at iENA 2018 for his invention, "Programmable Spectrum LED Light for Plant Cultivation," and a silver medal at the 45th Geneva Innovation Exhibition for the "Six-Spectral LED Solar Simulator." He holds a patent and a petty patent for a total of five inventions. He can be contacted at email: watjanatepin.n@gmail.com.